Materials Advances

ROYAL SOCIETY OF CHEMISTRY

PAPER

View Article Online
View Journal | View Issue

Cite this: *Mater. Adv.*, 2022, 3, 4718

Invariant electrical conductivity upon thermal ageing of a crosslinked copolymer blend for high voltage insulation†

Sarath Kumara,‡[a] Amir Masoud Pourrahimi,‡[b] Azadeh Soroudi,‡[b] Xiangdong Xu,*[a] Thomas Hammarström,[a] Yuriy Serdyuk[a] and Christian Müller *[b]

Received 10th February 2022,
Accepted 19th April 2022

DOI: 10.1039/d2ma00153e

rsc.li/materials-advances

Click chemistry type reactions between polyethylene-based copolymers are a promising and by-product free alternative to peroxide crosslinking of low-density polyethylene, which is widely used as an insulation material for high-voltage power cables. Here, the impact of thermal ageing on the long-term stability of the thermo-mechanical and dielectric properties of a copolymer blend is evaluated that can be cured through a by-product free reaction between the epoxy and carboxylic acid functional groups attached to the polyethylene backbone. It is observed that ageing at 90 °C in air for up to 2500 h does not affect the direct current (DC) electrical conductivity of about 3×10^{-14} S m^{-1}, provided that a suitable antioxidant is added that prevents the thermo-oxidative degradation of the polyethylene backbone. Furthermore, the material maintains its thermo-mechanical properties upon ageing such as a high ductility at room temperature and a stiffness of about 1 MPa above the melting temperature of polyethylene. Evidently, the use of click chemistry type reactions is a promising strategy for the design of new high-voltage insulation materials that can be cured without the formation of by-products.

Introduction

The rapidly growing demand for electricity combined with the shift from fossil to renewable sources of energy requires efficient long-distance electric power transmission.[1,2] High-voltage direct current (HVDC) submarine and underground power cables are an integral part of future power grids that seamlessly integrate wind and solar farms as well as hydro-electric dams, all of which are often located in remote areas.[3,4] Such HVDC cables require an insulating layer with excellent dielectric and thermo-mechanical properties.[2,4]

Crosslinked low-density polyethylene (XLPE) is the most widely used insulating material for extruded HVDC cables. XLPE based insulating materials feature a low direct current (DC) electrical conductivity of $\sigma_{DC} \approx 2 \times 10^{-14}$ S m^{-1} at 70 °C – a typical cable operating temperature – and an electric field exposure of up to 20 kV mm^{-1}.[5,6] The insulating properties can be improved further by adding conductivity reducing additives, such as metal oxide nanoparticles,[7–9] conjugated polymers[10] and aromatic voltage stabilisers,[11–13] as well as a small amount of high-density polyethylene.[14]

XLPE based insulation materials are obtained by radical crosslinking of low-density polyethylene (LDPE) using peroxides such as dicumyl peroxide (DCP). The peroxide curing process results in by-products such as methane, acetophenone, cumyl alcohol, and α-methylstyrene,[15,16] which can increase the DC electrical conductivity and pose a potential health and safety hazard. Hence, by-products need to be removed, which is typically performed using a time and energy consuming degassing procedure.[17] As a result, strategies that reduce or avoid the generation of by-products during the crosslinking process are of great importance. One approach is to reduce the amount of peroxides that are needed for radical crosslinking, which can be achieved through the incorporation of vinyl groups.[18] Another strategy involves the development of insulation materials that can be cured through a click chemistry-type crosslinking reaction, which does not produce any by-products.[5,19–21]

Click chemistry-type crosslinking can be realised by using blends of polyethylene copolymers that comprise functional groups, which can undergo a curing reaction. We have previously studied blends of a statistical ethylene–glycidyl methacrylate copolymer, p(E-*stat*-GMA) and a statistical ethylene–acrylic acid copolymer, p(E-*stat*-AA) (see Fig. 1 for

[a] *Department of Electrical Engineering, Chalmers University of Technology, Gothenburg 41296, Sweden. E-mail: christian.muller@chalmers.se, xiangdong.xu@chalmers.se*
[b] *Department of Chemistry and Chemical Engineering, Chalmers University of Technology, Gothenburg 41296, Sweden*

† Electronic supplementary information (ESI) available. See DOI: https://doi.org/10.1039/d2ma00153e

‡ These authors contributed equally.

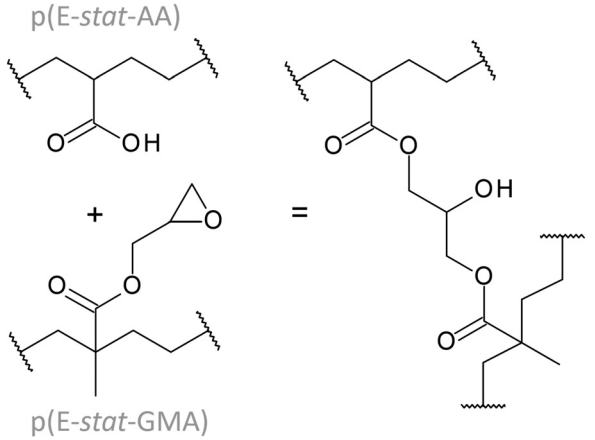

Fig. 1 Chemical structures of the branched statistical copolymers p(E-*stat*-AA) and p(E-*stat*-GMA) (left) as well as the covalent crosslink that forms upon the reaction of carboxylic acid and an epoxy group (right).

chemical structures).[5,19] These two types of copolymers can be compounded at, *e.g.*, 120 °C, which lies above their respective melting temperatures of $T_m \approx 108$ °C and 101 °C. Heating to temperatures above 140 °C triggers the curing reaction that leads to the formation of a covalent crosslink (Fig. 1).[5] The cured blends display a DC electrical conductivity of about 1×10^{-14} S m^{-1} measured at 70 °C and 20 kV mm^{-1} provided that the overall comonomer content is sufficiently low.[5,6] It is of paramount importance that the excellent dielectric properties of click chemistry-cured copolymer blends do not deteriorate with time. Ageing of polyethylene-based insulation materials can introduce chemical defects as well as structural changes, which can negatively affect their dielectric and thermo-mechanical properties[22–26] and hence may cause electrical treeing as well as a decrease in the dielectric breakdown strength.[27–30]

Here, we study how long-term ageing at 90 °C – the currently highest HVDC cable operating temperature – for up to 2500 h influences the dielectric and thermo-mechanical properties of a cured copolymer blend comprising p(E-*stat*-GMA) and p(E-*stat*-AA). We found that the electrical conductivity is not affected by ageing provided that a suitable antioxidant is added.

Experimental

Materials

The branched statistical copolymer p(E-*stat*-GMA) with a glycidyl methacrylate (GMA) content of 4.5 wt%, a melt flow index (MFI) of ~2 g (10 min)$^{-1}$ (190 °C/2.16 kg, data provided by the supplier), and a density of 0.93 g cm^{-3} was obtained from Arkema (Lotader series). The branched statistical copolymer p(E-*stat*-AA) with an acrylic acid (AA) content of 3.1 wt%, an MFI of ~10.6 g (10 min)$^{-1}$ (190 °C/2.16 kg, data provided by the supplier), and a density of 0.93 g cm^{-3} was obtained from SK Primacor Europe. Irganox 1010 was purchased from Sigma Aldrich and used as received.

Processing and sample preparation

Blends of p(E-*stat*-GMA) and p(E-*stat*-AA) with a stoichiometric ratio of 1.2 : 1 wt% : wt% were compounded for 10 min at 120 °C using a twin-screw Xplore Micro Compounder MC5. Irganox was added by first compounding a blend containing 1 wt% Irganox (one gram of antioxidant per 100 grams of the blend + antioxidant), which was diluted to 0.1 wt% through a second compounding step. The extrudate was first melted at 140 °C in a hot press, then cured at 200 °C for 10 min and finally cooled to room temperature, resulting in 0.3 mm thick films. The samples were then aged at 90 °C in air using a UN55 universal oven from Memmert.

Attenuated total reflectance (ATR) Fourier-transform infrared (FTIR) spectroscopy

FTIR spectra were recorded using a PerkinElmer FTIR spectrophotometer equipped with a GladiATR attachment from Pike Technologies. Each spectrum was obtained by averaging 32 scans.

Differential scanning calorimetry (DSC)

DSC thermograms were recorded under nitrogen (50 mL min^{-1}) from 20 to 150 °C at a heating/cooling rate of 10 °C min^{-1}, using a Mettler Toledo DSC2 instrument and a TC-125MT intercooler. The sample weight was 2–4 mg. Thermo-oxidative degradation was monitored at 190 °C by first keeping the sample for 5 min under nitrogen gas flow and then switching to air flow.

Dynamic mechanical analysis (DMA)

DMA thermograms were recorded from 30 to 200 °C using a TA Q800 instrument in tensile mode at a heating rate of 3 °C min^{-1}, a pre-load strain of 0.01%, a maximum strain of 0.05% and a frequency of 0.5 Hz. The samples with dimensions of $12.7 \times 5.8 \times 0.3$ mm^3 were cut from melt-pressed films.

DC conductivity measurements

The leakage currents were measured at 30, 50 and 70 °C using a test cell based on a three-electrode system, which consisted of a high voltage electrode, a grounded guard ring electrode, and a circular measuring electrode with an area of 6.16 cm^2. The electrode system was connected to a high-voltage power supply (Glassman FJ60R2) and a DC voltage of 6 kV was applied across the 0.3 mm thick specimen resulting in an electric field level of 20 kV mm^{-1} for 12 h. The volume leakage current was recorded using a Keithley 6517B electrometer and the LabView based dynamic average software. The DC electrical conductivity σ_{DC} was calculated based on the close to steady state leakage currents obtained at the end of the 12 h time interval.

Dielectric frequency response

Frequency domain spectroscopy (FDS) was carried out using an insulation diagnostic analyser IDAX 300 in combination with a high voltage amplifier VAX020. Material specimens (0.3 mm in thickness) were measured at 2 kV peak-to-peak and a frequency

range from 0.1 mHz to 1 kHz at three temperatures, 30 °C, 50 °C and 70 °C. The loss tangent was calculated based on the measured complex capacitance (see ref. 6 for details).

Results and discussion

We chose to work with two copolymers, p(E-*stat*-GMA) and p(E-*stat*-AA), with low comonomer contents of 4.5 wt% GMA and 3 wt% AA, respectively. Blends of the two copolymers were compounded at 120 °C, one without any antioxidant and a second type that contained 0.1 wt% Irganox 1010, followed by curing at 200 °C (see the Experimental section for details).

In a first set of experiments, we recorded differential scanning calorimetry (DSC) isotherms at 190 °C in air to determine the extent of thermo-oxidative degradation. For the cured blend, we observe the onset of an exothermic degradation process as soon as air is introduced (Fig. 2). The deviation from the isothermal baseline after the gas switch suggests the immediate degradation of the cured blend that does not contain the antioxidant with an oxidation induction time (OIT) of 0 min. In most significant contrast, the isotherm recorded for the cured blend containing 0.1 wt% Irganox features a significantly reduced exotherm at $t > 5$ min which suggests that the OIT exceeds the duration of the experiment (OIT > 30 min), indicating that the antioxidant can largely suppress thermo-oxidative degradation.

The cured blend samples were aged at 90 °C for 500 to 2500 h at ambient atmosphere, and Fourier-transform infrared (FTIR) spectroscopy was performed to investigate the chemical processes that underlie the observed thermo-oxidative degradation of the cured blend without the antioxidant. The as-cured blend features two absorption peaks at 1705 cm^{-1} and 1735 cm^{-1} prior to ageing (Fig. 3a), which we assign to the stretching vibrations of carbonyl groups that are part of (1) carboxylic acid dimers and (2) the ester of GMA or the covalent crosslink, respectively (see Fig. 1).[19] The cured blend containing Irganox features a more pronounced absorption at 1735 cm^{-1} relative to the absorption at 1705 cm^{-1}, when compared to the cured blend without the antioxidant. The more extensive consumption of carboxylic acid groups is consistent with a higher degree of crosslinking as discussed below.

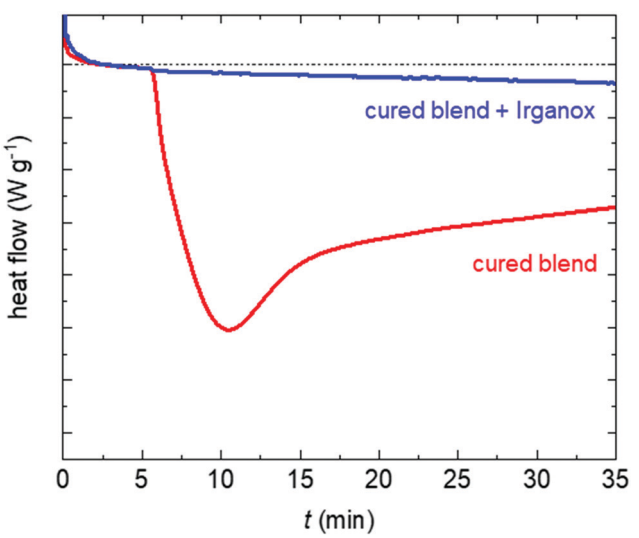

Fig. 2 DSC isotherm at 190 °C under an air flow ($t > 5$ min) for the cured binary blend without the antioxidant (red) and the cured binary blend with 0.1 wt% Irganox (blue).

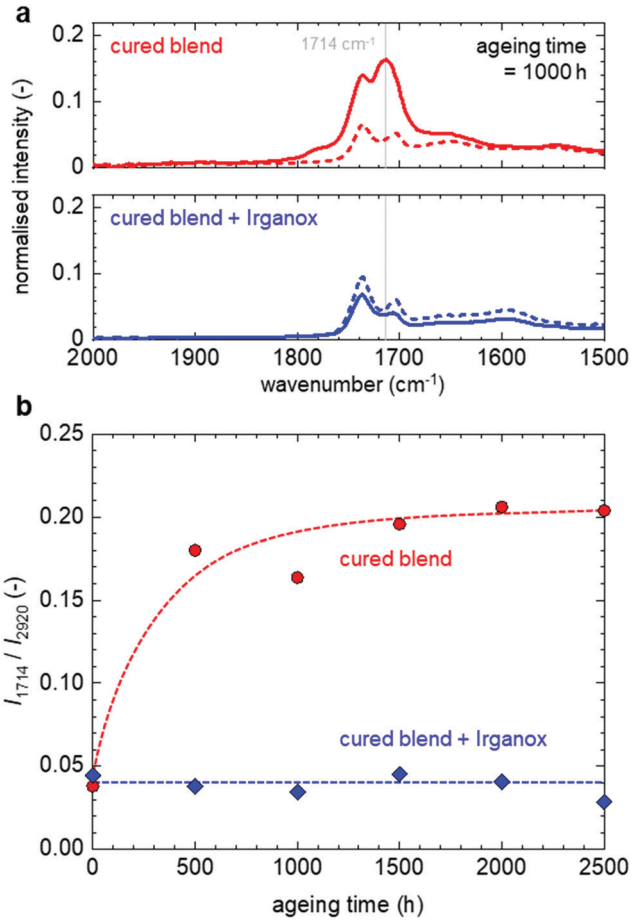

Fig. 3 (a) FTIR spectra of the cured binary blend without (red) and with 0.1 wt% Irganox (blue) prior to ageing (dashed lines) and after ageing for 1000 h (solid lines) and (b) absorbance at 1714 cm^{-1} normalised by the absorbance at 2920 cm^{-1}, corresponding to the asymmetric C–H stretching of the cured binary blend without (red) and with Irganox (blue).

In the case of blends without the antioxidant, a distinct new absorption peak emerges at 1714 cm^{-1} upon ageing, which we assign to the stretching vibrations of carbonyl groups that are introduced to the polyethylene backbone in the form of ketones as a result of thermo-oxidative degradation (Fig. 3a).[31–33] Instead, ageing did not significantly affect the FTIR spectra of the cured blend with the antioxidant (Fig. 3a), indicating that the presence of 0.1 wt% Irganox is able to suppress the oxidation of the cured blend. We used the absorption at 1714 cm^{-1} to monitor the thermo-oxidative degradation at 90 °C (Fig. 3b). The samples without the antioxidant underwent rapid thermo-oxidative degradation already during the first 500 hours of ageing while the samples with the antioxidant

featured an invariant FTIR absorption in the carbonyl region up to 2500 h of ageing at 90 °C. The OIT of samples containing 0.1 wt% Irganox and aged for up to 2000 h was longer than 30 min (the same as samples prior to ageing, see Fig. 2), while, for an ageing time of 2500 h, an OIT of about 5 min was obtained (Fig. S1, ESI†). This observation indicates that the material contained a sufficient amount of antioxidant to hinder thermo-oxidation for at least 2500 h of ageing at 90 °C. It is expected that a higher content of Irganox 1010 would increase the OIT of the material aged for 2500 h.

Dynamic mechanical analysis (DMA) was used to investigate how ageing influences the storage modulus E' of the materials. The DMA thermograms of the samples aged for 1000 h are characteristic for the cured blends (Fig. 4a). Both materials display a considerable decrease in stiffness above the melting temperatures of the two copolymers, p(E-*stat*-GMA) and p(E-*stat*-AA), *i.e.* $T_m \approx 108$ °C and 101 °C.[5] The cured binary blend features a rubber plateau above the melting temperature with a value of $E_p \approx 0.2$ MPa in the case of the cured blend without the antioxidant, while the Irganox-containing blend shows a higher value of $E_p \approx 1$ MPa after 1000 h of ageing. The rubber plateau modulus can be used to estimate the molecular weight between network points (network points can be crosslinks, trapped entanglements, *etc.*) according to $M_c = \rho RT/E_p$, where $\rho = 0.789$ cm^{-3} is the density of polyethylene at $T = 140$ °C. We obtain values of 13.5 kg mol^{-1} and 2.7 kg mol^{-1} for the cured blend without and with Irganox (consistent with the FTIR spectra of the cured blends; see Fig. 3a), which corresponds to 1 and 5 network points per 1000 carbons, respectively, *i.e.* comparable to a previously obtained value of 3.5 network points per 1000 carbons for the same curing time and temperature.[5] The two copolymers p(E-*stat*-AA) and p(E-*stat*-GMA) have a comonomer-to-ethylene ratio of 1 : 108 GMA : E and 1 : 83 AA : E, respectively, which implies that the complete consumption of all functional groups would give rise to about 5 crosslinks per 1000 carbons. We have previously shown that the cured blends of p(E-*stat*-AA) and p(E-*stat*-GMA) contain not only covalent crosslinks but also a significant fraction of physical network points in the form of (trapped) entanglements.[19]

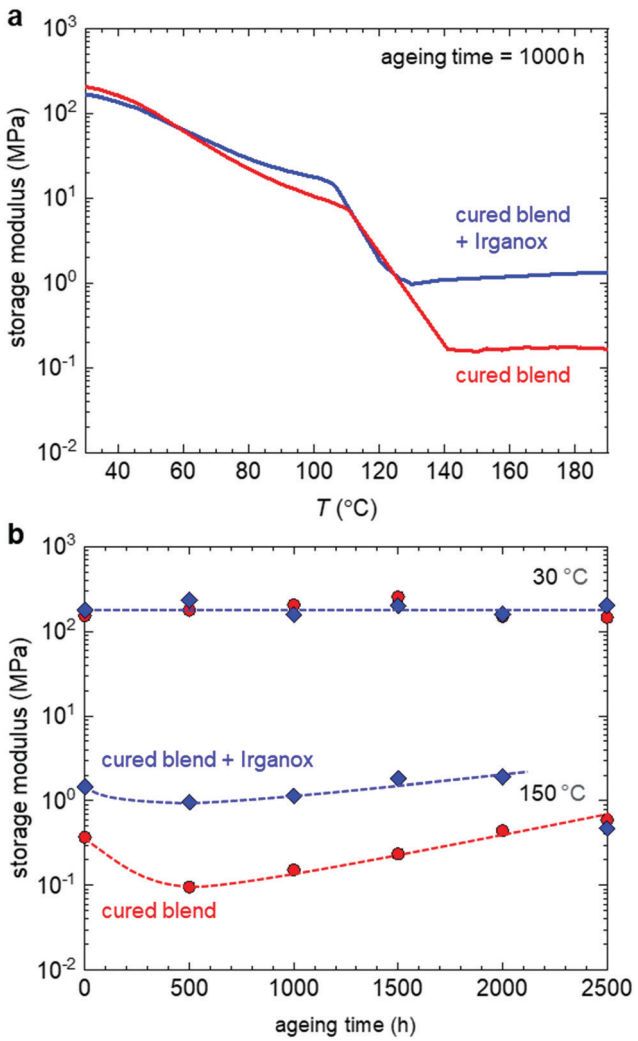

Fig. 4 (a) DMA thermograms of the samples aged for 1000 h and (b) storage modulus *versus* ageing time at 30 °C and 150 °C of the cured binary blend without (red) and with 0.1 wt% Irganox (blue).

To explore whether ageing alters the stiffness of the materials, the storage moduli at 30 °C and 150 °C were plotted *versus* the ageing time. The storage modulus below the melting temperature was unaffected by ageing (Fig. 4b). This observation is consistent with an invariant crystallinity of about 30%, as determined by DSC (ESI† Fig. S2). The rubber plateau modulus of the cured blend, with and without antioxidant, first decreased upon ageing for 500 h but then gradually increased upon ageing for longer times. We argue that ageing at 90 °C, which is close to the melting temperature of the copolymers, facilitates the reorganisation of at least some physical network points, leading to a slight decrease in the rubber plateau. More long-term ageing, however, leads to a gradual increase in the rubber plateau because the curing reaction slowly proceeds at the chosen annealing temperature.

To investigate the impact of ageing at 90 °C on the dielectric properties of the cured blends, leakage currents were recorded at 70 °C and 20 kV mm^{-1}. The leakage current of the cured blends that did not contain the antioxidant significantly increased by more than two orders of magnitude as a result of ageing, while the cured blends with Irganox displayed an invariant leakage current (Fig. 5a). The DC electrical conductivity was calculated based on the leakage current measured after 12 h. The cured blend without the antioxidant features a low σ_{DC} of 2×10^{-14} S m^{-1} at 70 °C and 20 kV mm^{-1} (Fig. 5b; see ESI† Fig. S3 for measurements at 30 °C and 50 °C), which is comparable to the σ_{DC} of LDPE measured under the same conditions.[5] The cured blend with Irganox only had a slightly higher value of $\sigma_{DC} \approx 3 \times 10^{-14}$ S m^{-1}, which we assign to the presence of the antioxidant.[34] The DC electrical conductivity of the cured blend without the antioxidant strongly increased with ageing time, reaching a value of $\sigma_{DC} \approx 2 \times 10^{-11}$ S m^{-1} after 1000 h at 90 °C. In contrast, the cured blend containing Irganox displayed the same DC electrical conductivity up to at least 2500 h of ageing at 90 °C.

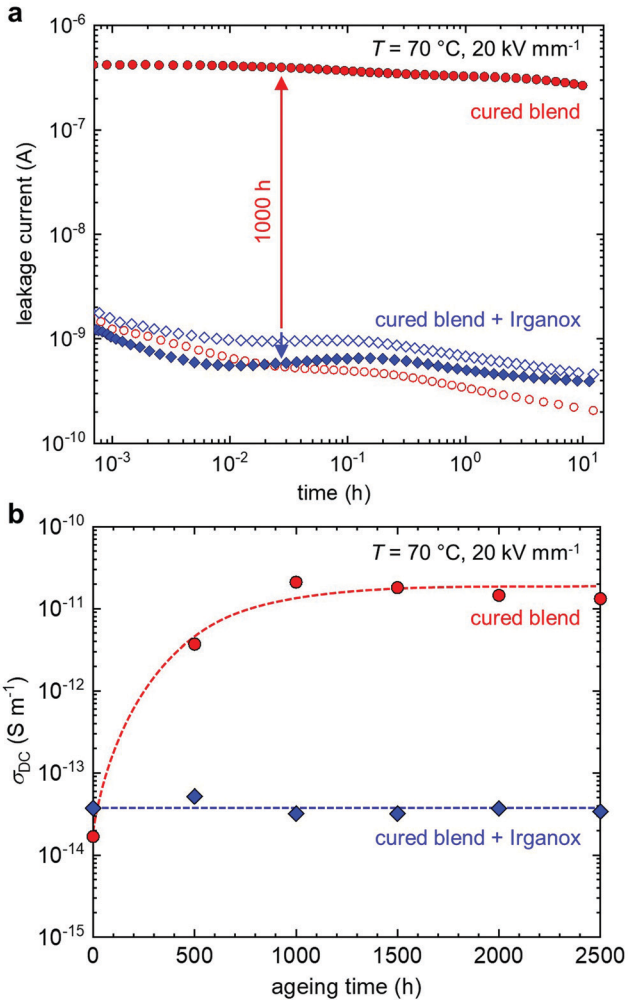

Fig. 5 (a) Leakage current recorded at 70 °C and 20 kV mm^{-1} for the cured binary blend without (red) and with 0.1 wt% Irganox (blue) prior to ageing (open symbols) and after ageing for 1000 h (full symbols) and (b) DC electrical conductivity σ_{DC} at 70 °C and 20 kV mm^{-1} as a function of ageing time calculated from charging currents at 12 h.

In a final set of experiments, frequency domain spectroscopy (FDS) was carried out to study the frequency dependence of the dielectric response from 0.1 mHz to 1 kHz from which the loss tangent was determined (Fig. S4, ESI†). We found that for the cured blend without antioxidant the loss tangent at 50 Hz increases with ageing time, *e.g.* from about 5×10^{-4} to 3×10^{-3} at 70 °C after 2500 h of ageing at 90 °C (Fig. S5, ESI†). Instead, the loss tangent recorded for the binary blend with the antioxidant only slightly changed upon ageing, *e.g.* from about 4×10^{-4} to 6×10^{-4} under the same conditions. Evidently, the presence of 0.1 wt% Irganox can prevent the degradation of the dielectric properties up to at least 2500 h.

Conclusions

We have investigated the impact of ageing at 90 °C and air on the thermo-mechanical and dielectric properties of a cured blend composed of a statistical ethylene–glycidyl methacrylate copolymer, p(E-*stat*-GMA), and a statistical ethylene–acrylic acid copolymer, p(E-*stat*-AA). Curing of the blend proceeds *via* a click chemistry-type reaction between epoxy and carboxylic acid functional groups, resulting in a thermoset material with a DC electrical conductivity of $\sigma_{DC} \approx 2 \times 10^{-14}$ S m^{-1}, which is comparable to the σ_{DC} of LDPE. Ageing of the cured blend results in thermo-oxidative degradation, which does not strongly influence the thermo-mechanical properties, as measured with DMA, but leads to a significant increase in σ_{DC} by more than two orders of magnitude. The addition of the antioxidant Irganox 1010 results in a slightly higher σ_{DC} of $\approx 3 \times 10^{-14}$ S m^{-1} prior to ageing, which however does not change upon ageing for at least 2500 h, which is consistent with the suppression of thermo-oxidative degradation as inferred from FTIR spectroscopy. Evidently, click chemistry type curing of the copolymer blend studied here is a promising alternative for insulation materials based on peroxide-crosslinked LDPE.

Conflicts of interest

There are no conflicts to declare.

Acknowledgements

We gratefully acknowledge the Chalmers Area of Advance Energy and the Swedish Foundation for Strategic Research (grant agreement no. FFL 15-0147) for financial support.

References

1 G. C. Montanari, P. H. F. Morshuis, M. Zhou, G. C. Stevens, A. S. Vaughan, Z. Han and D. Li, *High Voltage*, 2018, **3**, 90–95.
2 G. Mazzanti and M. Marzinotto, *Main Principles of HVDC Extruded Cable Design*, Wiley IEEE Press, New York, 2013.
3 A. Purvins, L. Sereno, M. Ardelean, C.-F. Covrig, T. Efthimiadis and P. Minnebo, *J. Clean. Prod.*, 2018, **186**, 131–145.
4 H. Ye, T. Fechner, X. Lei, Y. Luo, M. Zhou, Z. Han, H. Wang, Q. Zhuang, R. Xu and D. Li, *High Voltage*, 2018, **3**, 79–89.
5 M. Mauri, A. I. Hofmann, D. Gómez-Heincke, S. Kumara, P. Amir Masoud, Y. Ouyang, P.-O. Hagstrand, T. Gkourmpis, X. Xu, O. Prieto and C. Müller, *Polym. Int.*, 2020, **69**, 404–412.
6 S. Kumara, X. Xu, T. Hammarström, Y. Ouyang, A. M. Pourrahimi, C. Müller and Y. V. Serdyuk, *Energies*, 2020, **13**, 1434.
7 A. M. Pourrahimi, T. A. Hoang, D. Liu, L. K. H. Pallon, S. Gubanski, R. T. Olsson, U. W. Gedde and M. S. Hedenqvist, *Adv. Mater.*, 2016, **28**, 8651–8657.
8 B. Nageshwar Rao and V. S. Nandakumar, *Mater. Today: Proc.*, 2019, **18**, 994–1005.
9 A. M. Pourrahimi, R. T. Olsson and M. S. Hedenqvist, *Adv. Mater.*, 2018, **30**, 1703624.

10 A. M. Pourrahimi, S. Kumara, F. Palmieri, L. Yu, A. Lund, T. Hammarström, P.-O. Hagstrand, I. G. Scheblykin, D. Fabiani, X. Xu and C. Müller, *Adv. Mater.*, 2021, **33**, 2100714.
11 Y. Shi, X. Chen, F.-B. Meng, Z. Hong, M. Awais and A. Paramane, *ACS Appl. Polym. Mater.*, 2022, **4**, 1422–1430.
12 X. Chen, A. Paramane, H. Liu, J. Tie, Z. Wei and Y. Tanaka, *Polym. Eng. Sci.*, 2020, **60**, 717–731.
13 X. Chen, L. Yu, C. Dai, A. Paramane, H. Liu, Z. Wei and Y. Tanaka, *IEEE Trans. Dielectr. Electr. Insul.*, 2019, **26**, 2041–2049.
14 M. G. Andersson, J. Hynynen, M. R. Andersson, V. Englund, P.-O. Hagstrand, T. Gkourmpis and C. Müller, *ACS Macro Lett.*, 2017, **6**, 78–82.
15 A. Smedberg, T. Hjertberg and B. Gustafsson, *Polymer*, 1997, **38**, 4127–4138.
16 J. Sahyoun, A. Crepet, F. Gouanve, L. Keromnes and E. Espuche, *J. Appl. Polym. Sci.*, 2017, 134.
17 T. Andrews, R. N. Hampton, A. Smedberg, D. Wald, V. Waschk and W. Weissenberg, *IEEE Electr. Insul. Mag.*, 2006, **22**, 5–16.
18 V. Englund, J. Andersson, J.-O. Boström, V. Eriksson, P.-O. Hagstrand, J. Jungqvist, W. Loyens, U. H. Nilsson and A. Smedberg, *CIGRE Session*, Paris, D1.104, 2014.
19 M. Mauri, A. Peterson, A. Senol, K. Elamin, A. Gitsas, T. Hjertberg, A. Matic, T. Gkourmpis, O. Prieto and C. Müller, *J. Mater. Chem. C*, 2018, **6**, 11292–11302.
20 M. Mauri, L. Svenningsson, T. Hjertberg, L. Nordstierna, O. Prieto and C. Müller, *Polym. Chem.*, 2018, **9**, 1710–1718.
21 M. Mauri, N. Tran, O. Prieto, T. Hjertberg and C. Müller, *Polymer*, 2017, **111**, 27–35.
22 J. C. Fothergill, G. C. Montanari, G. C. Stevens, C. Laurent, G. Teyssedre, L. A. Dissado, U. H. Nilsson and G. Platbrood, *IEEE Trans. Dielectr. Electr. Insul.*, 2003, **10**, 514–527.
23 C. Kim, P. Jiang, F. Liu, S. Hyon, M.-G. Ri, Y. Yu and M. Ho, *Polym. Test.*, 2019, **80**, 106045.
24 S. Tantipattarakul, A. S. Vaughan and T. Andritsch, *High Voltage*, 2020, **5**, 270–279.
25 Y. Zhang, Z. Hou, K. Wu, S. Wang, J. Li and S. Li, *Materials*, 2020, **13**, 2056.
26 X. Dai, J. Hao, Z. Jian, R. Liao, X. Zheng and Y. Zhang, *High Voltage*, 2021, DOI: **10.1049/hve1042.12139**.
27 A. Mantsch, X. Chen, J. Blennow and S. Gubanski, *Proceedings of 23rd Nordic Insulation Symposium*, Norway, 2013.
28 X. Chen, A. R. Mantsch, L. Hu, S. M. Gubanski, J. Blennow and C. O. Olsson, *IEEE Trans. Dielectr. Electr. Insul.*, 2014, **21**, 45–52.
29 X. Chen, Y. Xu, X. Cao and S. Gubanski, *IEEE Trans. Dielectr. Electr. Insul.*, 2015, **22**, 2841–2851.
30 Y. Y. Zhang, S. T. Li, J. Gao, S. H. Wang, K. N. Wu and J. Y. Li, *IEEE Trans. Dielectr. Electr. Insul.*, 2020, **27**, 1795–1802.
31 C. Strandberg, L. Burman and A. C. Albertsson, *Eur. Polym. J.*, 2006, **42**, 1855–1865.
32 K. Grabmayer, G. M. Wallner, S. Beissmann, U. Braun, R. Steffen, D. Nitsche, B. Roder, W. Buchberger and R. W. Lang, *Polym. Degrad. Stab.*, 2014, **109**, 40–49.
33 M. Da Cruz, L. Van Schoors, K. Benzarti and X. Colin, *J. Appl. Polym. Sci.*, 2016, **133**, 43287.
34 M. E. Karlsson, X. Xu, H. Hillborg, V. Ström, M. S. Hedenqvist, F. Nilsson and R. T. Olsson, *RSC Adv.*, 2020, **10**, 4698–4709.